EDDY CURRENT CURVILINEAR SCANNED LINEAR ARRAY NEAR REAL-TIME IMAGING TECHNIQUE

H. Dale Collins and R. Parks Gribble

Battelle, Pacific Northwest Laboratories
P. O. Box 999
Richland, WA 99352

INTRODUCTION

This paper describes work by Battelle, Pacific Northwest Laboratories (Battelle Northwest) to assist General Dynamics/Convair to meet its general requirement for near real-time nondestructive evaluation (NDE) of cruise missile surfaces and components using rotary scanned eddy current imaging techniques.

Small surface defects (i.e., cracks) of critical size located in the cruise missile skin, may propagate under severe stress cycling in flight and result in mission failure. The loss or failure, as a result of critical crack propagation, of these strategic and tactical weapons can be circumvented if a cost-effective, viable inspection system is available during the manufacturing and testing phases.

The present inspection technique requires leviathan immersion tanks filled with dye penetrant liquid, etc. Cruise missile fuselages are then immersed and subjected to dye penetrant tests for surface crack detection and evaluation.

This procedure is extremely time consuming, requiring extensive operator experience, large quantities of dye penetrant solution, costly decontamination procedures, etc.

The impetus of the work at Battelle Northwest was to prove feasibility of surface crack inspection using high resolution/real-time rotary scanned eddy current imaging techniques.

This goal was achieved in this phase of the program. Unique eddy current images of actual fatigue cracks in aluminum cruise missile material were obtained.

GENERAL DESCRIPTION OF THE LABORATORY EDDY CURRENT CURVILINEAR SCANNED IMAGING SYSTEM FOR CRUISE MISSILES

The basic imaging system consists of single-frequency current sources driving the sense and reference coils integrated with the co-

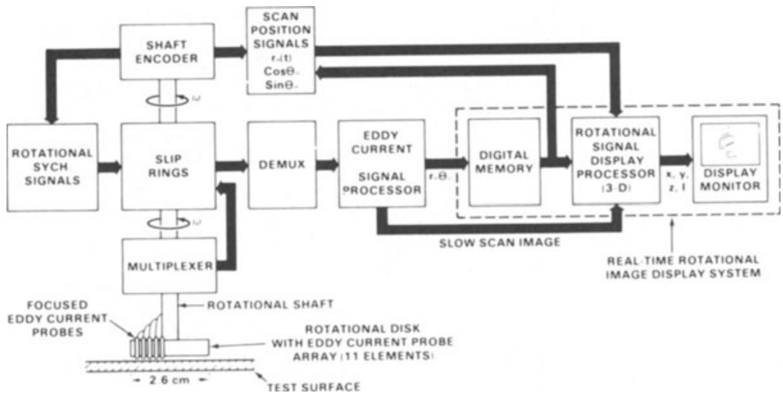

Fig. 1. Eddy current rotary scanner focused probe array imaging system.

herent signal processor. The system is structured to provide focused probe eddy current images with 3-D format. The simplified block diagram of the eddy current rotary imaging system is shown in Fig. 1.

A variable speed rotary scanner is used to acquire eddy current image data. Each coil in the array is attached to a spring-loaded mechanism to eliminate spurious motion and lift-off during rotation (see Fig. 2). The eddy current bridge containing the ten coils is

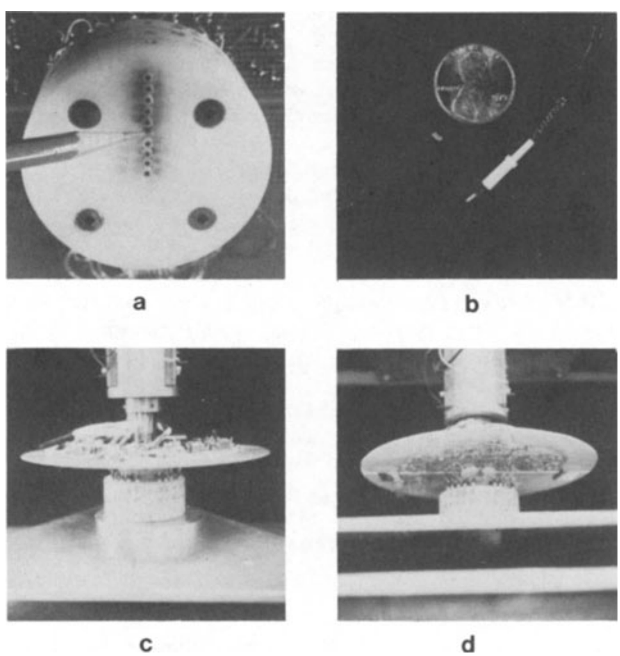

Fig. 2. Laboratory rotary eddy current scanning system: a) scanning head with 10 discrete coils; b) imaging coil and holder; c) and d) rotary disk and slip rings.

structured to produce maximum signals in air at the differential amplifier output. The receiver output (i.e., object signal) and reference signal are applied to a phase sensitive amplitude detector or amplitude detector in the signal processor.

Curvilinear Eddy Current Coil Array

Fig. 3 shows a linear array of ten discrete eddy current focused coils on a rotational disk. Each coil is approximately 1.45 mm in diameter. The linear array generates 20 discrete raster lines across the diameter of the disk. The sampling increment in the radial direction is approximately 2.5 mm or 1.4 wavelengths in aluminum at 100 kHz. The sampling frequency and disk velocity determine the sampling increment along each of the 10 discrete circular paths of different radii. The path lengths vary directly as a function of the radius and equal sampling requires the sample rate to decrease as the path radius decreases.

The maximum sampling frequency is directly proportional to the inspection frequency. The general rule or criterion is to sample at least 10 cycles of the inspection frequency per coil. At 100 kHz inspection frequency, the maximum sampling frequency is 10 kHz. A line of ten coils would then require 1 ms sampling time. If a line is sampled every 1 degree of rotation, then 360 lines are generated every revolution, thus requiring 36×10^{-3} seconds (i.e., 36 ms).

Fig. 4 is a graph illustrating the relationship between the sampling increment and sampling rate for various disk rotation speeds. The graph represents the outer circular path on the 5 cm diameter aperture. The inner paths will always have sufficient sampling if the sampling criterion for the outer path is satisfied.

The dotted line represents the 0.5 mm sampling interval for various disk rotation speeds and sampling times. If the sampling time (ts) remains constant at 100 μsec/coil and we increase the disk rotation

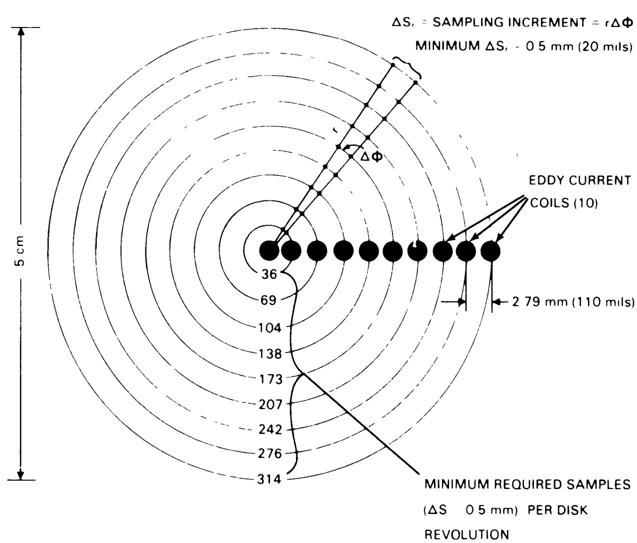

Fig. 3. Curvilinear eddy current imaging disk and coil array.

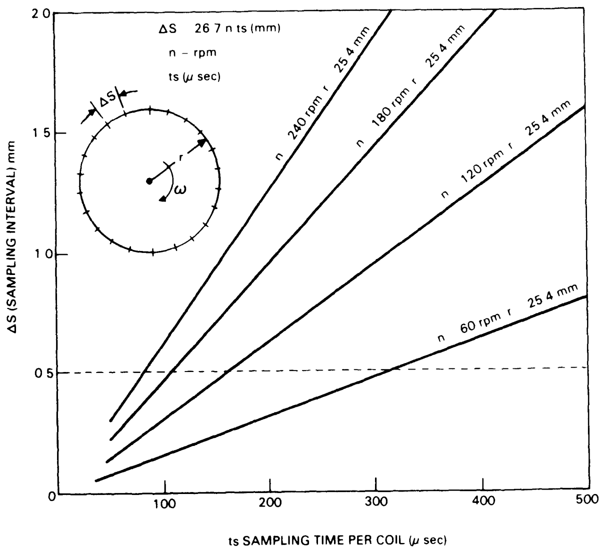

Fig. 4. Coil sampling interval versus sampling time for curvilinear imaging.

speed from 60 to 180 rpm, the sampling interval increases from 0.16 mm to approximately 0.5 mm. Thus, variable sampling density is achieved by simply varying the rotation speed!

This feature is very desirable because in the search mode, the inspection rate can be three to four times greater than the high resolution mode (i.e., minimum sampling). The operator simply increases or decreases the disk rotation speed to achieve variable sampling.

Eddy Current Focused Probe Image Resolution in Aluminum

Image resolution as a function of object-to-probe distance, effective aperture, and frequency is an extremely important parameter to verify experimentally. The distance (ΔX) is defined as the minimum resolvable separation between two object points. The two-point resolution criterion has long been used as a quality factor for optical and acoustical imaging systems.

Fig. 5 shows the resolution aluminum test block and the associated eddy current images in 3-D format. Fig. 5a is the test block with various slot separations between 0 mm to 18.0 mm simulating a series of two line objects (or cracks) in cruise missile material. The resolvable line images will then determine the eddy current probe resolution. Fig. 5c is the C-scan view of the resolution block and the line separations 4.0 mm, 3.0 mm, 2.0 mm, and 1.5 mm are resolvable. Hence, the probe resolution is approximately 1.5 mm which is essentially one wavelength in aluminum at 100 kHz illumination.

Fig. 5b, 5d, and 5e illustrate the unique 3-D images of the resolution slots with the front surface. The slot widths appear larger in the image as a result of the 1.5 mm lateral resolution. These slots simulate a 0.25 mm wide crack in aluminum.

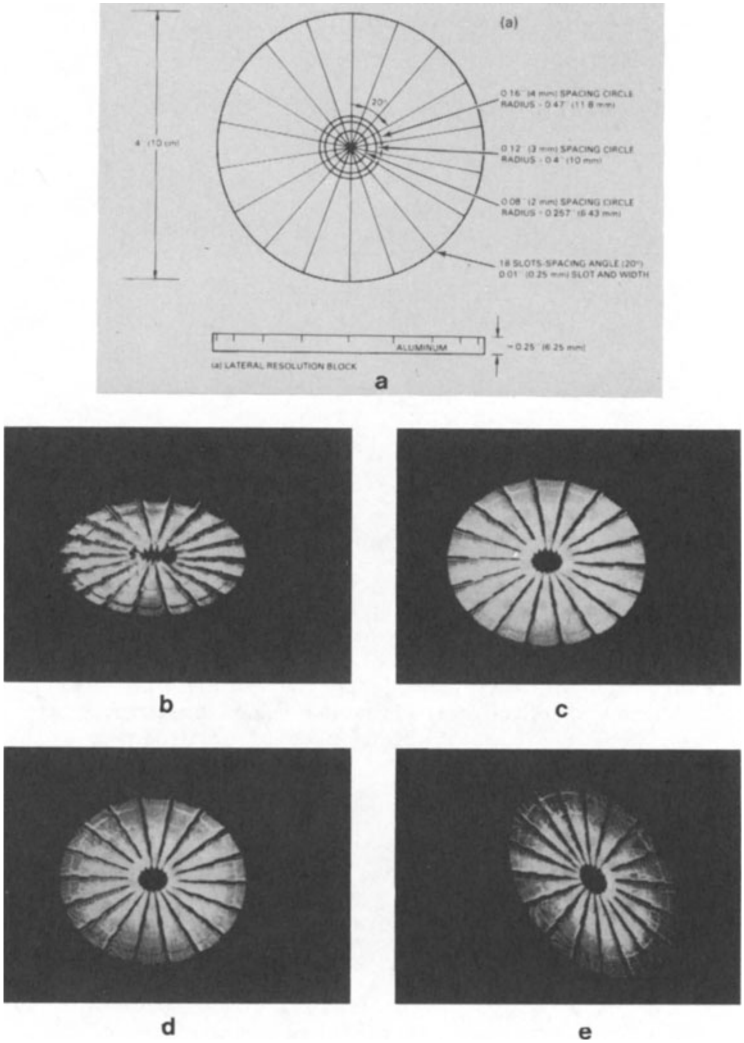

Fig. 5. Eddy current resolution test block and associated images: a) test block of simulated radial cracks; b)-e) 3-D images of the radial slots using only 10 discrete coils.

Depth resolution can be achieved by system calibration and microprocessor calculation of object phase versus slot depth. Phase look-up tables could then be generated and stored in EPROM and used to generate the "Z" position signal in the 3-D processor.

EXPERIMENTAL RESULTS USING ALUMINUM CRUISE MISSILE COMPONENTS AND ALUMINUM PLATES

A series of experiments were conducted to evaluate the following parameters with respect to cruise missile inspection:

Image Resolution (i.e., surface cracks)

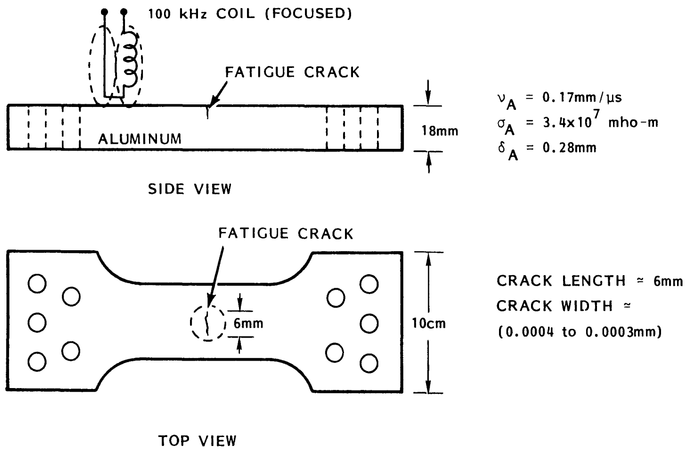

Fig. 6. Fatigue crack geometry in aluminum.

- Image Display
- Real-Time Inspection.

The results graphically illustrate the unique eddy current images that were obtained with the curvilinear scanned systems. Various simulated and real defects (i.e., fatigue cracks) in cruise missile aluminum were imaged with success.

Fatigue Crack (6 mm) in Aluminum

Fig. 6 is the eddy current image construction geometry of a small surface fatigue crack in aluminum. The crack length is approximately 6 mm and the variable width between 0.4 and 3 microns. The depth appears to be greater than 0.25 mm.

Fig. 7a is a photograph of the fatigue crack specimen with the crack located within the circular outlined section.

Fig. 7b is a photo-microscope picture of a small section with the 10 micron division scale. The approximate crack width can be determined using this scale. A large number of small surface scratches are revealed in this photograph and will provide a background image clutter for the crack. The results show dramatically the effect of small surface scratches is negligible.

Fig. 7c shows the crack with a 0.4 mm division scale. The length is easily calculated to be approximately 6 mm.

Fig. 8 is a series of under-sampled eddy current 3-D images of the fatigue crack. The inspection frequency was 100 kHz and the probe resolution approximately 1.5 mm. The surface breaking crack is easily viewed against the upper block surface in Fig. 8a, b, c, and d. The length-width ratio appears distorted as a result of the lateral resolution.

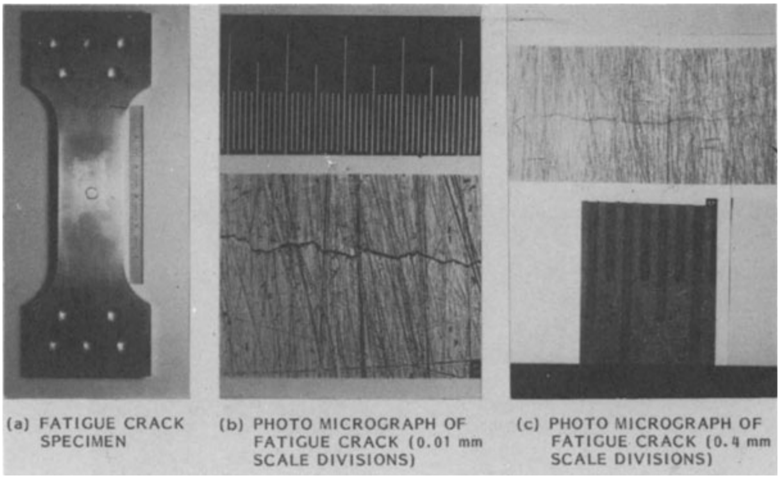

Fig. 7. Optical photographs of the fatigue crack in aluminum.

The coarse line density is the result of only 10 discrete coils on the rotating disk.

Fig. 9a, b, and c are eddy current 3-D images of the fatigue crack simulating 50 discrete coils across the disk radius. The images exhibit excellent resolution graphically illustrating the effects of optimum sampling.

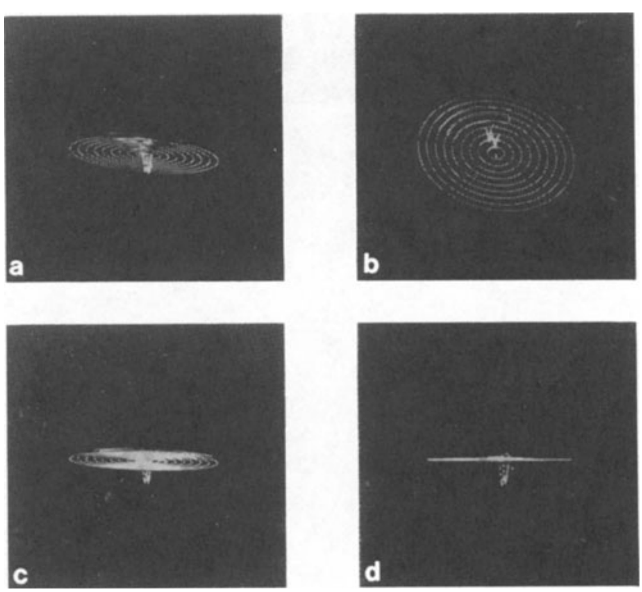

Fig. 8. Eddy current 3-D images of the fatigue crack using only 10 discrete coils (i.e., 2.5 mm sampling).

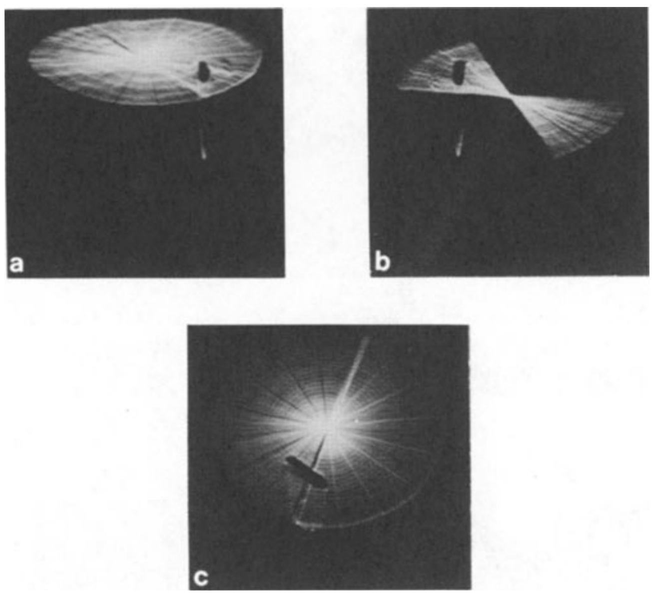

Fig. 9. Curvilinear scanned 3-D eddy current images of a fatigue crack simulating 50 discrete coils (i.e., 0.5 mm sampling).